Regulation and modulation of growth : insights from human and animal studies

Gool, S.A.van

Chapter 4

Marginal growth increase, altered bone quality and polycystic ovaries in female prepubertal rats after treatment with the aromatase inhibitor exemestane

S.A. van Gool[1], J.M. Wit[1], T. de Schutter[2], N. de Clerck[2], A.A. Postnov[2], S. Kremer Hovinga[1], J. van Doorn[3], S.J. Veiga[4], L. Miguel Garcia-Segura[4], M. Karperien[5]

[1]Department of Pediatrics, Leiden University Medical Center, Leiden, the Netherlands.
[2]Department of Biomedical Sciences and Department of Physics, University of Antwerp, Antwerp, Belgium.
[3]Department of Metabolic and Endocrine Diseases, University Medical Center Utrecht, Utrecht, the Netherlands.
[4]Instituto Cajal, Consejo Superior de Investigaciones Científicas, Madrid, Spain.
[5]Department of Tissue Regeneration, Biomedical Technology Institute, Twente University, the Netherlands.

Hormone Research in Paediatrics 2010;73(1):49-60

Abstract

Background: Aromatase inhibition has been proposed as a potential approach for growth enhancement in children with short stature, but detailed animal studies are lacking.

Aim: to assess the effect and potential adverse effects of aromatase inhibition on growth in female rats.

Methods: Prepubertal Wistar rats received intramuscular injections with placebo (PLC) or the aromatase inhibitor exemestane at a dose of 10, 30 or 100 mg/kg/week (E10, E30, E100) for 3 weeks. A control group was ovariectomized (OVX). Weight and length gain, tibia and femur length, growth plate width, organ weights, insulin-like growth factor I (IGF-I) levels, and histology of the ovaries, uterus, and brain were analyzed. X-ray microtomography of femora was performed.

Results: E100 significantly increased weight gain and growth plate width, but less prominently than OVX. Trabecular number and thickness were decreased in E100 and OVX in the metaphysis and epiphysis. E100 significantly decreased ovarian weight and multiple cysts were seen upon histological evaluation. No significant effects were found on IGF-I levels and brain morphology in E100. E10 and E30 had no effects on growth.

Conclusion: a high dose of exemestane marginally increases axial and appendicular growth in female rats, at the expense of osteopenia and polycystic ovaries.

Introduction

Estrogens play a pivotal role in the regulation of normal skeletal growth and maturation in both boys and girls (1-5). In both genders, estrogen deficiency due to mutations in the aromatase gene (6) leads to the absence of a pubertal growth spurt, ongoing growth into adulthood and potentially tall stature. Based on these clinical observations, it was postulated that estrogen deficiency induced by aromatase inhibition, could be valuable in clinical practice because of its potential growth-enhancing effect (7;8).

Treatment with the nonsteroidal aromatase inhibitor letrozole resulted in an increased predicted adult height in boys with idiopathic short stature (ISS) (9;10) in two clinical trials performed by the group of Dunkel *et al.* In one of those trials, treatment with a combination of letrozole and testosterone increased near-final height in boys with a constitutional delay of puberty (11). There is limited experience with the use of aromatase inhibitors in female patients with short stature, since therapy-induced hyperandrogenism and consequent virilization may be expected, as observed in female aromatase-deficient patients. However, it is uncertain whether treatment with aromatase inhibition limited to the prepubertal period, with the objective to increase longitudinal growth and adult height, would cause persistent virilization and disturbance of reproductive function after cessation of treatment.

In girls with McCune-Albright syndrome (MAS) (12;13) or congenital adrenal hyperplasia (CAH) (14), treatment with the aromatase inhibitor testolactone or letrozole resulted in attenuated height velocity and bone maturation rates, resulting in a poor adult height prediction. These results are in conflict with the potentially growth-enhancing effect of aromatase inhibition in boys with ISS, but may also be the reflection of the complex endocrine deregulation in MAS and CAH patients. The reported clinical trials in girls were uncontrolled, and usually did not include an evaluation of bone mineral density (8).

The broad tissue distribution of aromatase expression in humans underscores the importance of locally produced estrogens (15). Therefore, aromatase inhibition for the purpose of growth enhancement may have side effects on several organ systems. Aromatase-deficient females are diagnosed with 46,XX DSD (disorder of sex development) at birth and show progressive bone age delay, eunuchoid proportions, and reproductive dysfunction based on primary amenorrhea and enlarged, polycystic ovaries in adolescence (6). Bone mineral density has not been studied in these patients, but one could hypothesize that they would develop osteoporosis, as it occurs in adult men with congenital estrogen deficiency (2). Treatment of adolescents girls with a gonadotropin releasing hormone agonist (GnRHa), an alternative way to diminish circulating estrogen levels, indeed resulted in a decreased bone mineral density (16). Moreover, aromatase expression plays an important role in the brain under both physiological and pathological

conditions (17). Aromatase inhibition may also have an impact on the brain, since aromatase expression was found to have a neuroprotective role both under physiological and pathological conditions (17).

In the present article, we report the results of a study in which female sexually immature rats were treated with the steroidal, irreversible aromatase inhibitor exemestane (E) in a slow-release preparation in order to test the hypothesis that aromatase inhibitors can increase longitudinal growth and to evaluate potential side-effects. Treatment was short-term and confined to the period of sexual immaturity in order to mimic the potential treatment strategy in girls with ISS.

We chose to work with exemestane in our experiments, because it can be administered once a week as a slow release preparation to ensure long-lasting aromatase inhibition, in contrast to the other available aromatase inhibitors that have to be administered daily. This facilitates its use in experimental animal models, and it presumably would also increase compliance in clinical practice. A second advantage of exemestane over the other aromatase inhibitors is that it irreversibly inactivates aromatase and completely abolishes estrogen biosynthesis, which can only be overcome by de novo synthesis of aromatase. We applied a slow release depot of exemestane to continuously counteract de novo synthesis of aromatase. Finally, exemestane may exhibit androgenic effects on bone, potentially preventing the loss of bone mineral density (BMD) induced by estrogen deficiency (18), which may be an advantage when treatment with aromatase inhibitors is considered in clinical practice.

In addition to the effects of aromatase inhibition on growth, we also studied possible adverse effects of aromatase inhibition on bone physiology, brain morphology, and morphology of the ovaries and uterus. This study is the first detailed analysis of the impact on growth and potential side effects of aromatase inhibition in a female animal model.

Experimental design

Animals

Weight-matched female Wistar rats (n=30) were purchased from Harlan (Horst, The Netherlands). At the start of the experiments, all rats were 26 days old, and sexually immature, since rats usually enter sexual maturation at the age of 30 days. Animals were kept in a light and temperature controlled room (12 hours light, 20-22°C) with water and food (Hope Farms, Woerden, The Netherlands) ad libitum and a maximum of 3 animals per cage. Experiments were approved by the Committee for the ethical care and use of laboratory animals of the Leiden University.

Five groups consisting of 6 rats were formed. One group was ovariectomized at baseline by the dorsal approach under isoflurane anaesthesia in order to obtain an estrogen-deficient control group (OVX). In previous experiments, no difference in growth phenotype was found between sham-operated and placebo-treated control-group rats (19). Therefore, no sham-group was included in this study. Three groups were treated with the slow-release preparation exemestane (Aromasin® provided by Pfizer, New York, U.S.A) at a dose of 10, 30 or 100 mg/kg body weight/week (coded as E10, E30, E100, respectively). Exemestane was administered by intramuscular injections in alternated hind paws. A control group was treated with vehicle (placebo, PLC). After three weeks of treatment, all rats were sacrificed.

Weekly measurements of nose-anus length, tail length and body weight were performed. At the end of the experimental period, animals were anaesthetized by intraperitoneal Nembutal injection and blood samples were collected by means of cardiac puncture. Serum was separated for insulin-like growth factor I (IGF-I) measurements. Femora were collected for X-ray microtomography (micro-CT). Subsequent *in vivo* fixation was performed by means of transcardiac perfusion with 4% paraformaldehyde and 0.2% glutaraldehyde in 0.1 M phosphate buffer supplemented with 75 mM lysine monohydrochloride and 10 mM Na-periodate. After fixation, the rats were decapitated, and the brains were stored in the same fixative for at least 12 weeks. Tibiae of the right hind legs were measured, postfixated for 24 hours, decalcified in 12.5 % EDTA, pH 7.4 for 4 weeks, cut in halves in a sagittal orientation and subsequently processed for paraffin embedding. Ovaries and uterus were weighed and processed for paraffin embedding. The organ weight/total body weight (TBW) ratio was calculated.

Growth plate histomorphometry

For histomorphometrical analysis of the growth plate, paraffin sections (5 µm) perpendicular to the growth plate axis were mounted on APES/glutaraldehyde-coated slides, and deparaffinized in Paraclear® and graded ethanols. They were stained with Haematoxylin/Eosin (H&E) and mounted in Histomount (National Diagnostics, Atlanta, USA). Representative pictures of the proximal tibial growth plate were taken (Nikon DXM 1200 digital camera). Widths of the total growth plate, proliferative zone and hypertrophic zone were measured in ImagePro Plus®. The ratio between proliferative and hypertrophic zone widths (P/H ratio) was calculated.

X-ray microtomography (micro-CT)

To examine the effects of exemestane treatment on whole bone parameters and on trabecular bone in particular, right femora were analyzed by high resolution X-ray microtomography. Micro-CT has been shown to be well suited for the non-destructive visualization and quantitative analysis of bone and calcified tissue (20;21).

a. 'Whole bone' parameters

Isolated whole femora were scanned with a high resolution desktop micro-CT scanner (Skyscan 1076, Kontich, Belgium). In this X-ray micro-CT system, both the X-ray source (focal spot size 5 µm, energy range 20-100 keV) and the detector (CCD camera 2.3kx4k) rotate around the bone. Scans were isotropic and a voxel size of 35×35×35 µm was chosen with 1.0 mm A1 filter. Virtual cross-sections were reconstructed by Feldkamp cone-beam algorithm (22). Further technical details about the scanner have been published elsewhere (23).

The same threshold and reconstruction parameters were used for the reconstruction of all cross-sections. Frequency distribution of the grey levels was analyzed. 3D models were created using Skyscan software packages ANT and CT Analyzer. From the virtual cross-sections the volumes taken by bone as well as the anatomical volume (Archimedean volume) were calculated. Distinction between bone and other tissues was based on thresholding of the grey values in the reconstruction. Analysis of the grey values in the individual slices also resulted in a relative value for total calcium and overall calcium density. Details of these calculations have been reported previously (20). In addition, the length of the femora was measured manually with a caliper.

b. Trabecular bone

For analysis of the trabecular bone, the distal end of the femur was scanned, but for this purpose at a higher resolution than required for the 'whole bone' scans. Therefore, an *in vitro* desktop micro-CT system (Skyscan 1072, Kontich, Belgium) with a rotating stage was used (24). Polychromatic X-rays, with peak energy of 80 kV, were generated by a microfocus X-ray source with a focal spot size of 8 microns. A (1024×1024) 12 bit CCD camera was used as detector. In all experiments the rotation step was 0.9°, acquisition time 6 sec/projection, and total acquisition time about 2 hours. Scanning was isotropic with a voxel size of 13 μm^3.

The growth plate was chosen as a reference for selecting comparable and reproducible regions of interest for analysis of trabecular bone parameters such as trabecular number, trabecular thickness, bone volume and distribution of trabecular thickness. Trabecular bone parameters were studied in two different regions of the femur: the metaphysis (primary ossification center)

and the epiphysis (secondary ossification center). For analysis of the primary ossification center at the proximal side of the growth plate, a transverse reference slice of the growth plate was selected and used to reconstruct a cylinder with fixed dimensions as from 50 slices above the reference slice; the height of the cylinder was 150 slices.

Gonadal histology

Midsagittal sections of the ovaries (5 µm) were stained with Haematoxylin and Eosin (H&E). A minimum of three sections was analyzed per ovary. In H&E stained longitudinal sections (5 µm) of the uterus, endometrial thickness was measured using ImagePro Plus® and the endometrium/total wall thickness ratio (E/T-ratio) was calculated.

Brain histology

Brains were removed from the skulls, rinsed with PBS and cut in coronal sections (30 µm) in a Vibratome. Sections were Nissl-stained with toluidine blue for screening morphometrical analysis of all brain areas. Immunohistochemical staining of astrocytes (anti-GFAP, Glial Fibrillary Acidic Protein, DAKO, Barcelona, Spain; diluted 1:1000), microglia (OX-42, Serotec, Bicister, United Kingdom; diluted 1:300) and reactive astrocytes (anti-vimentin, clone V9, DAKO, Barcelona, Spain; diluted 1:500) was performed. For the morphometric analysis of GFAP immunoreactive astroglia, a quantitative evaluation of the surface density of GFAP immunoreactive cell bodies and cell processes in the hippocampus was performed using a stereological grid, according to the point-counting method of Weibel (25). For each animal, a minimum of two slides was evaluated.

Insulin-like Growth Factor I (IGF-I) assay

Total serum IGF-I levels were measured by specific radioimmunoassay (RIA) after acid Sep-Pak C18 (Waters Associates Ltd., Milford, MA) extraction of 250 µl aliquots, following procedures as described previously (26).

Statistical analysis

The study was designed to analyze the effect of aromatase inhibition on growth and to analyze potential adverse effects on bone, brain and organ development. Comparisons of growth among treatment and control groups were made using one-way analysis of variance (ANOVA). Results are expressed as mean and SD. The significance level was set at 0.05.

Results

Effects on growth and organs

At baseline, there were no significant differences between groups in auxological parameters. Body weight gain, nose-anus length gain and tail length gain, tibia length, growth plate characteristics, and IGF-I levels are summarized in table 1. The effects of aromatase inhibition on organ weights are summarized in table 2. Figure 1 illustrates nose-anus length gain in OVX, PLC and E100. Figure 2 shows growth plate samples from these groups. Results in the E10 and E30 groups were not significantly different from the placebo-group and are therefore not presented.

Body weight gain was significantly increased in both E100 and OVX ($p=0.000$ and $p=0.001$, respectively) compared with PLC. Nose-anus length gain was significantly higher ($p=0.000$) in OVX compared with PLC. Figure 1 illustrates that the increased length gain in OVX was already prominent one week after ovariectomy. A less pronounced increasing nose-anus length gain with a trend towards statistical significance ($p=0.054$) was seen in the E100 group. The difference in nose-anus length gain between OVX and E100 was statistically significant ($p=0.021$). When compared to the rats that received placebo-treatment, for both E100 and OVX no effect on tail length gain was found. Total growth plate width in the E100 group was increased ($p=0.000$), based on equal thickening of both the proliferative and hypertrophic zones compared with PLC. The P/H ratio was not significantly different from controls. Similar effects were found in OVX. The serum IGF-I level was raised in OVX ($p=0.000$), but not significantly in E100, compared to PLC.

In the OVX group, a significant decrease of 15% of the liver/TBW ratio was found ($p=0.042$). The increased thymus/TBW ratio found in OVX ($p=0.000$), was not seen in the E100 group.

Table 1: Effect of aromatase inhibition on growth parameters and epiphyseal morphology

Parameter	PLC	E100	OVX
Tail length gain (cm)	7.2 (0.7)	7.3 (0.4)	7.9 (0.5)
Nose-anus length gain (cm)	5.0 (0.7)	5.7 (0.8)$^{\#\,\wedge}$	6.5 (0.4)***
Body weight gain (g)	96.7 (10.2)	120.6 (7.3)***	115.0 (7.6)**
Tibia length (mm)	30.7 (0.4)	31.2 (0.7)$^{\#\,\wedge}$	31.7 (0.3)**
Femur length (mm)	26.6 (0.4)	27.6 (0.4)*	27.0 (0.2)
Growth plate width (mm)	0.34 (0.02)	0.42 (0.02)***	0.44 (0.02)***
proliferative zone (mm)	0.14 (0.01)	0.18 (0.01)***	0.18 (0.01)**
hypertrophic zone (mm)	0.20 (0.02)	0.24 (0.02)*	0.26 (0.02)**
P/H-ratio	0.70 (0.05)	0.77 (0.1)§	0.67 (0.05)
Serum IGF-I (ng/ml)	0.9 (0.04)	1.1 (0.16)$^{\wedge}$	1.4 (0.25)*

Means (SD). E100 or OVX versus PLC: *p<0.05; **p<0.01; ***p<0.001; $^{\#}$p<0.1.
E100 versus OVX: $^{\wedge}$p<0.05; §p<0.1.

Table 2. Effect of aromatase inhibition on organ weights

Parameter	PLC	E100	OVX
liver	70.9 (10.8)	70.3 (6.3)§	59.7 (11.1)*
thymus	2.9 (0.4)	3.3 (0.5)$^{\wedge\wedge}$	4.0 (0.5)***
kidney	5.5 (0.3)	5.8 (1.1)§	5.1 (0.6)
adrenal gland	0.23 (0.04)	0.19 (0.05)$^{\#\wedge}$	0.23 (0.03)
ovary	0.2 (0.03)	0.1 (0.02)***	
uterus	2.6 (0.8)	2.1 (0.9)$^{\wedge\wedge\wedge}$	0.2 (0.04)***
endometrium thickness (µm)	0.43 (0.10)	0.31 (0.10)$^{*\,\wedge\wedge}$	0.14 (0.05)***
total wall thickness (µm)	0.75 (0.06)	0.57 (0.12)$^{**\,\wedge\wedge}$	0.26 (0.09)***
E/T-ratio	0.57 (0.11)	0.54 (0.11)	0.57 (0.09)

Organ weights as permillage of total body weight. Means (SD). E/T-ratio, ratio between endometrium thickness and thickness of the total uterus wall.
E100 or OVX versus PLC: *p<0.05; **p<0.01; ***p<0.001; $^{\#}$p<0.1.
E100 versus OVX: $^{\wedge}$p<0.05; $^{\wedge\wedge}$p<0.01; $^{\wedge\wedge\wedge}$p<0.001; §p<0.1.

Figure 1

Changes in nose-anus length gain in PLC, E100 and OVX during the experimental period.

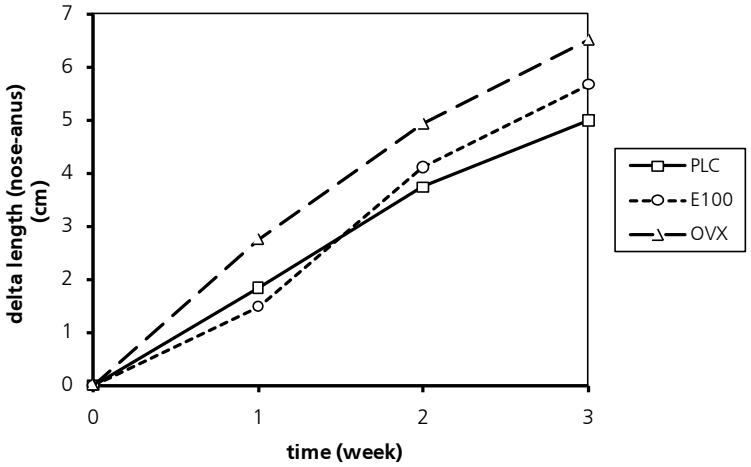

Figure 2

Growth plate samples from PLC, E100 and OVX. Notice the increase in total growth plate width in E100 and OVX.

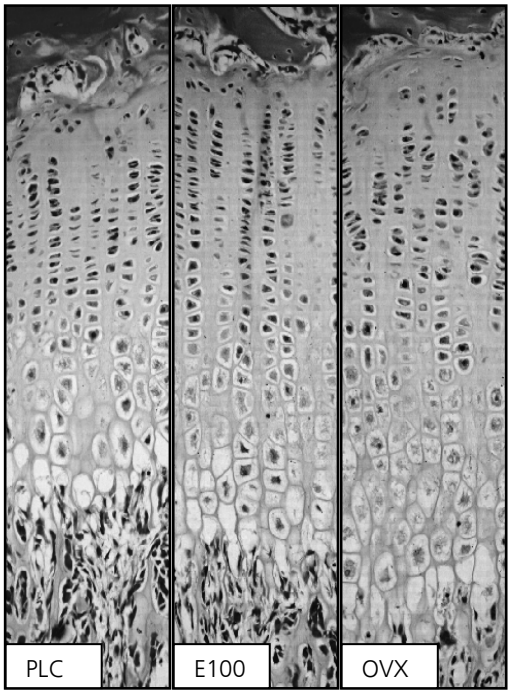

Effects on bone

a. 'Whole bone' parameters

Femur length was significantly increased in E100, but not in OVX, whereas tibia length was significantly higher in OVX only. Observed changes between groups in calcium density, total calcium, bone volume and anatomical volume did not reach statistical significance (table 3).

b. Trabecular bone analysis

As illustrated in table 4, a clear reduction of trabecular number and trabecular thickness was apparent in both the epiphysis and the metaphysis of OVX and E100 as compared to PLC ($p<0.05$). Figure 3A shows the trabecular volume distribution of trabeculae with a given thickness, corrected for the bone volume that was studied in the epiphysis. Notice that the percentage of thin trabeculae (<5.0 pixels) was increased whereas the percentage of thick trabeculae (>5.0 pixels) was decreased in OVX and E100. A similar, but more pronounced effect on the distribution of trabecular thickness was observed in the metaphysis or primary ossification center (fig. 3B). As expected, the trabeculae in the metaphysis were thinner than in the epiphysis.

Effect on ovaries and uterus

E100 caused a statistically significant decrease of 50% of the ovary/TBW ratio ($p=0.000$). No statistically significant difference in the uterus/TBW-ratio was found, but the ratio was significantly decreased in OVX with 92% ($p=0.000$). Both endometrial thickness and the total thickness of the uterus wall were significantly decreased in E100 and OVX, resulting in normal endometrium thickness/total wall thickness ratios compared with PLC.

Ovaries from placebo-treated controls contained follicles in various stages of development (fig.4A), including secondary follicles, mature Graafian follicles and corpora lutea, the latter confirming the occurrence of ovulation. Similar histological characteristics were seen in the ovaries of E10- and E30-treated rats (data not shown). The ovaries from the E100-treated group also showed different developmental stages of the follicle, but corpora lutea were absent and there were less mature follicles, demonstrating the absence of ovulation (fig. 4B). Instead, large cystic follicles, surrounded by a thin granulosa cell layer or no granulosa at all, were abundantly present.

Table 3. Whole bone parameters

Parameter	PLC	E100	OVX
Va: anatomical volume (mm^3)	277.8 (8.3)	287.3 (7.4)	279.2 (14.5)
Vb: bone volume (mm^3)	95.5 (4.4)	97.1 (5.1)	90.8 (5.1)
Vb/Va-ratio (%)	34	34	33
Total calcium	1.00	0.97	0.85
Calcium density	1.00	0.89	0.85

Means (SD). PLC was taken as a reference for calculating relative total calcium and relative calcium density.

Table 4. Trabecular bone analysis

Parameter		PLC	E100	OVX
Epiphysis				
Trabecular bone volume	mm3	25.6 (1.4)	22.4 (1.6)*^	20.2 (1.8)*
Trabecular thickness	µm	143.1 (1.0)	139.4 (2.3)*	139.6 (3.2)*
Trabecular number	1/mm	1.8 (0.0)	1.6 (0.2)* ^	1.4 (0.1)*
Metaphysis				
Trabecular bone volume	mm3	2.5 (0.4)	1.9 (0.3)*	1.8 (0.3)*
Trabecular thickness	µm	85.1 (3.3)	75.9 (2.9)*	78.5 (3.1)*
Trabecular number	1/mm	3.6 (0.5)	3.0 (0.3)*	2.9 (0.4)*

Trabecular bone volume is the volume taken by trabecular bone in the selected region of interest.
Means (SD); *$p<0.05$ as compared to PLC; ^$p<0.05$ E100 versus OVX.

Figure 3

(A) Normalized trabecular volume distribution in the secondary ossification center (epiphysis). Only the volume taken by bone tissue in the epiphysis is taken into account. Notice the increase of trabeculae <5.0 pixels (pixel size = 27.64 µm). (B) Normalized trabecular volume distribution in the primary ossification center (metaphysis). Only the volume taken by bone tissue in the selected cylinder is taken into account. Notice the increase of trabeculae <5.0 pixels (pixel size = 13.82 µm). *p <0.05.

A. Epiphysis

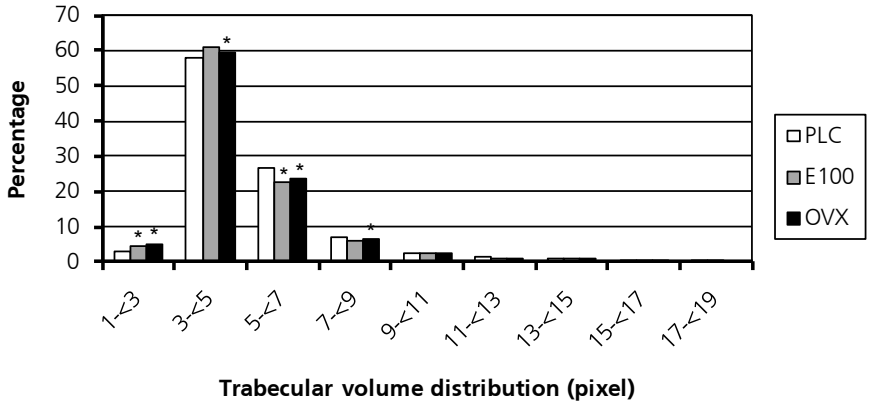

B. Metaphysis

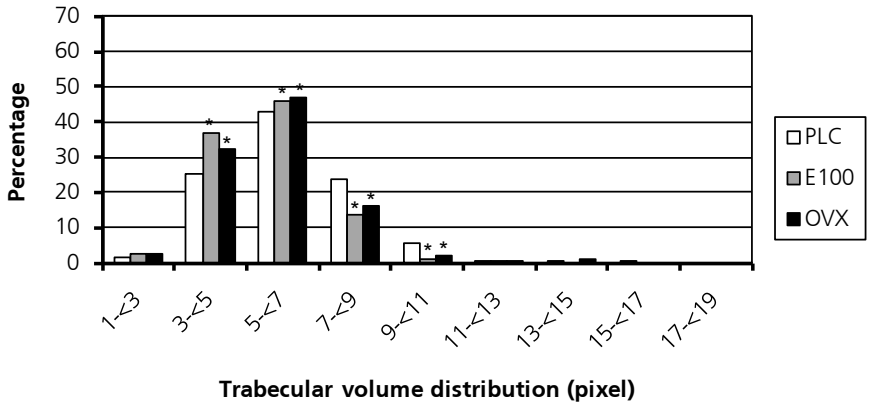

Figure 4

Ovaries of PLC (A) and E100 (B); GF, mature Graafian follicle; CL, corpus luteum; C, cyst; OD, ovarian duct. Magnification 40×. Notice the presence of cysts and the absence of corpora lutea in E100.

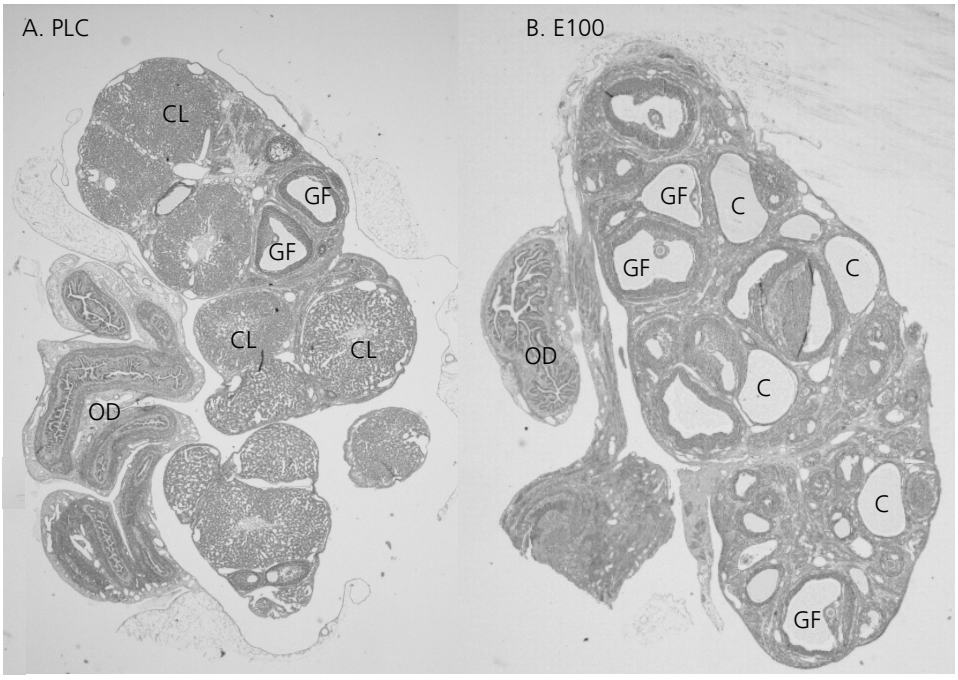

Brain histology

Histological examination of the brain was performed on slides of the hilus of the hippocampus area on E100 and placebo-treated animals to assess for possible neurodegenerative effects of the treatments. Since neurodegeneration is associated with gliosis, immunohistochemical staining for several glial markers was performed. There was no statistically significant difference in the surface area of GFAP immunoreactive astrocytes between groups. No reactive astrocytes or reactive microglia were detected after vimentin and OX-42 immunostaining, respectively. In addition, there was no qualitative evidence of neuronal loss or degeneration (data not shown).

Discussion

The aims of this study were to investigate the effect of aromatase inhibition on growth parameters and to study potential side-effects of this treatment on organ weight development, bone, and brain morphology in sexually immature female rats. The main conclusion from this study is that the currently highest available dose of exemestane (100 mg/kg/week) partially inhibits aromatase activity, which causes only a marginal stimulation of length gain and appendicular growth, but also results in the appearance of multiple ovarian cysts and changes in bone architecture consistent with early stage osteopenia.

All the currently available animal models for studying longitudinal growth are in some way flawed since they do not fully represent the hallmarks of human growth, such as an obvious growth spurt at the beginning and epiphyseal fusion with growth arrest at the end of puberty. These processes are both mediated by the exclusive action of estrogen, as illustrated by the clinical phenotype of estrogen resistant or deficient patients (6). Although rodents do not clearly demonstrate these maturational phenomena, growth diminishes after sexual maturation with growth rates approximating zero. Rats tend to respond in a similar fashion as humans to estrogen, with estrogen deficiency stimulating growth and estrogen treatment causing growth arrest (27). In contrast, estrogen receptor (α/β/$\alpha\beta$) and aromatase knockout mice show a normal adult length (28-32), indicating that hormonal regulation of growth in mice is distinctly different than in humans and rats. We therefore feel that the rat is the most appropriate of the available animal models for *in vivo* studies on the impact of chemically induced aromatase deficiency.

To correlate the effects seen in our study to the degree of aromatase inhibition, it would have been valuable to assess serum levels of estradiol, testosterone, dihydrotestosterone (DHT), and exemestane. However, accurate methods for measurement of estradiol in rat serum are lacking (33). Available estradiol assays that are developed for analyzing human serum samples, are insufficiently sensitive for quantification of low estradiol levels (34). Treatment with exemestane even further complicates estradiol detection due to the fact that metabolites of the compound interfere with the available assays for measurement of gonadal steroids (35). To our knowledge, there is currently no laboratory experienced with estradiol serological measurements in exemestane-treated rats.

Alternatively, we used the ovary, a highly estrogen-dependent organ, as a biological readout system for the effect of exemestane. The observed ovarian phenotype characterized by the absence of corpora lutea and the presence of multiple cysts is similar to the ovarian phenotypes of the aromatase knockout mouse (ArKO) (36) and female estrogen receptor alpha and beta knockout mice (αERKO and βERKO) (28). Moreover, aromatase deficient female patients also

have reproductive dysfunction based on primary amenorrhea and enlarged, polycystic ovaries in adolescence (6). The observed changes in ovarian morphology convincingly demonstrate that a reduction in estradiol levels was achieved by the administration of exemestane in our model system.

Hyperandrogenism is likely to occur during treatment with aromatase inhibitors and may eventually lead to virilization, as reported in female patients with aromatase deficiency. In our study, exemestane treatment was applied short-term and was not expected to cause signs of hyperandrogenism. However, when considering a longer treatment period covering the period of sexual maturity, possible signs of virilization, such as masculine sexual behavior and disturbance of reproductive function, should be monitored during and after termination of treatment

The growth phenotype of E100-treated female rats shows similarities with other described animal models for estrogen deficiency. An increased body weight gain was also observed in female αERKO and αβERKO mice, and female ArKO mice (29-31;37), corresponding with an increased deposition of intra-abdominal adipose tissue, high leptin and cholesterol levels, and hyperinsulinism (38). An elevated body mass index has not been described in female patients with aromatase deficiency, but this is probably due to the fact that they have received estrogen treatment. In the present study, fat deposition, food intake and energy expenditure were not measured.

Nose-anus length gain in E100-treated rats was normal, but showed a trend towards a significant increase compared with non-treated controls. In female αERKO, βERKO, αβERKO and ArKO mice, adult length was found to be normal compared to wild-type mice (28-32). However, the βERKO mouse but has a tendency to slightly increased growth during the post-pubertal phase (31), whereas female ArKO mice show an increased length gain peripubertally (29;30). E100 treatment resulted in a marginal increase of the length of the tibia (not significant). Surprisingly, femur length was found to be significantly higher in E100 compared with PLC, in the absence of a similar and more pronounced effect after OVX. All other parameters were more dramatically influenced by OVX than by E100, and we have no explanation for the contrasting effects of OVX and E100 on femur length. However, our knowledge of the timing and regulation of growth in various bones is limited, and has not been studied in detail. Regional differences may exist, and aromatase inhibition may therefore result in various degrees of growth stimulation in different bones.

Increased appendicular growth was found in βERKO mice (31). In contrast, the other knockout mouse models either have normal or decreased growth of the femur and/or tibia (29-31). One must bear in mind that in our study exemestane was administered during a short timeframe, whereas inborn genetic mutations in knockout mice and human patients with estrogen

deficiency or resistance can influence growth during all stages of life, which may explain the differences in growth characteristics.

The OVX group was included as a control group, to be able to compare the results of exemestane-induced and ovariectomy-induced estrogen deficiency. Ideally, there would be a complete absence of circulating estrogen in both E100 and OVX. However, the differences in several parameters between the groups suggest that E100 did not completely abrogate estrogen biosynthesis. OVX induced increased levels of IGF-I, as reported before in ovariectomized rats and mice in other studies (39;40). A raised IGF-I level was also found after E100-treatment, but this effect did not reach statistical significance. Estrogen normally causes thymus atrophy (41), which in our experiments was strongly prevented by OVX and to a lesser extent by E100 (not significant). Similarly, a reduced weight of the liver was found in OVX females, whereas no reduced liver weight was found in E100. Circulating high levels of androgen may have had protective effects on these tissues, either by direct effects on target organs or maybe in part by aromatization to estrogen by residual aromatase activity. Since the gonads are the only organs capable of synthesizing androgen precursors in the rat, ovariectomy results in a combined estrogen and androgen deficiency, ruling out protective effects by circulating androgen in the OVX group.

E100 treatment had a similar, but less prominent effect on growth than OVX. The increase in nose-anus length gain in E100 was delayed compared with OVX, suggesting that at least one week is necessary to establish a steady-state plasma level of exemestane that is able to influence growth. The growth plate and the long bones of the appendicular skeleton seemed most sensitive to aromatase inhibition, resulting in effects similar to those seen after OVX. Axial skeletal growth was less stimulated by E100, compared with OVX. Differences in sensitivity for aromatase inhibition may reflect variability in local estrogen biosynthesis in various tissues resulting in different levels of aromatase inhibition. Second, some organs may be more accessible for exemestane penetration than others. Another possible explanation for the modest effect of E100 on longitudinal growth may be that the dosage was too low to achieve complete inhibition of aromatase activity at the systemic level or at the tissue level. However, preclinical studies have shown that a single subcutaneous dose of 30 mg/kg exemestane reduced ovarian aromatase activity in adult female rats with approximately 80% (E. di Salle, unpublished results). The absence of significant growth effects in E10 and E30 was presumably due to sub-pharmacological serum levels of exemestane.

Studies in mature, female rats have demonstrated that the steroidal aromatase inhibitor exemestane and its principal metabolite 17-hydroxyexemestane significantly prevent bone loss induced by OVX, based on androgenic actions of these compounds on bone. In contrast, the non-steroidal aromatase inhibitor letrozole, that has no structural relationship to androgens,

does not have such protective effects on bone in mature female rats (18;42). Analysis of the trabecular bone in both the epiphysis and metaphysis demonstrated a significant reduction in the number and thickness of trabeculae in E100 and OVX, associated with a non-significantly decreased calcium density in both groups. Loss of bone tissue is a sign of osteopenia, generally considered as the stadium preceding osteoporosis. Similarly, ArKO mice were found to have a decreased peak BMD, prominent osteopenia on plain film radiographs and decreased trabecular volume and thickness (29;30). A low BMD was also found in βERKO and αβERKO mice (31).

In our study, the bone phenotypes of E100 and OVX were very similar. This suggests that there is no apparent bone-protecting androgenic effect of exemestane and its principal metabolite 17-hydroxyexemestane in prepubertal rats treated for 3 weeks, in contrast to what was reported previously about mature rats treated for a period of 16 weeks (18;42). Exemestane was reported to have a very low binding affinity (0.22%) for the androgen receptor *in vitro* and a marginal androgenic activity (only 1% of that of testosterone propionate) *in vivo* in male castrated rats. Since androgen receptor expression is lower in the tibial epiphysis and metaphyseal bone in female rats compared to males, we expect the androgenic potency of exemestane in our model system to be even lower than 1% which makes pronounced androgenic effects of exemestane on growth unlikely. In line with this hypothesis is the fact that no protective androgenic effect of exemestane on bone quality was observed. The discrepancy between our study and the report by Goss *et al.* may be explained by the fact that during bone modeling that occurs in immature rats different regulatory pathways involving androgen signaling may play a role than during maintenance of bone quality in mature rats.

It is not clear whether the osteoporotic changes observed would lead to a permanently worse bone quality. As the growing skeleton is in a constant process of bone modeling, it remains to be seen whether osteoporotic changes induced in this period would render the mature skeleton more vulnerable to osteoporotic fractures. Patients with P-450 aromatase deficiency or estrogen receptor mutation have a low bone mass, which may result from not having achieved a normal peak bone mass during childhood growth and development of the skeleton (43). Estradiol treatment in those patients induced an increase in BMD (6).

The uterus/TBW ratio was decreased after OVX, but not significantly different after E100 treatment, probably due to incomplete aromatase inhibition at the tissue level. Studies in mature cycling rats treated with letrozole also revealed a decreased uterine weight (44). In female patients, aromatase deficiency results in reproductive dysfunction based on primary amenorrhea and enlarged polycystic ovaries in adolescence (45), emphasizing the pivotal role of estrogen in ovarian development (46). Similarly, E100 reduced ovary weight and caused histological changes similar to those seen in polycystic ovary syndrome. It is unknown whether

the effects of temporary estrogen deficiency on the female gonadal tract are reversible and, if not, whether these changes have an impact on fertility or sexual behavior.

In the mammalian nervous system, aromatase expression plays an important role in neural differentiation and plasticity, neuroendocrine functions, and (sexual) behavior (17), both under physiological and pathological conditions. We therefore have assessed whether aromatase inhibition affects morphology of the hippocampus, a brain area that is sensitive to estradiol levels (47). E100 did not result in reactive gliosis, one of the most prominent cellular responses of the central nervous system to neurodegeneration (48). This finding is in agreement with previous studies showing that adult ArKO mice have normal hippocampus morphology, although they are more susceptible to neurodegeneration than their wild-type littermates (49). Thus, although aromatase exerts a protective effect against neurodegenerative stimuli (50-52), its inhibition does not compromise neuronal survival under normal circumstances. However, we cannot exclude that aromatase inhibition may affect other brain regions, especially brain nuclei that develop during sexual maturation (e.g. the medial amygdala) (53).

In summary, partial inhibition of aromatase activity by E100 resulted in marginal stimulation of axial and appendicular growth in female prepubertal rats. Although aromatase inhibition was probably incomplete, pronounced adverse effects were found on ovarian histology and bone architecture, and it remains unclear whether these would have long-term, permanent consequences for reproduction and fracture risk, respectively. Our finding that E100 stimulates growth, albeit marginally, mimics to a certain extent the clinical phenotype in aromatase deficient female patients who exhibit tall stature if untreated (54). Species differences in dependency on estrogen signaling probably underlie the discrepancies found in growth phenotype between the aromatase inhibitor treated rats and mice, and estrogen-deficient patients described in literature. However, considering the potential side-effects on bone physiology and morphology of the ovaries, treatment with aromatase inhibitors in girls in clinical practice should not be advised.

Acknowledgements

The authors thank Ivo Que for supervision of experimental animal procedures and Cok Hoogerbrugge for supervision of IGF-I radioimmunoassays. We would like to thank prof. Dr. Anton Grootegoed and Mrs. Marja Ooms for sharing their expert opinion on gonadal histology and development with us. Pfizer (New York, USA) is gratefully acknowledged for supply of Aromasin® and financial support of the study. This project was supported in part by a grant from ZonMW, the Netherlands Organization for Health Research and Development, to S.A. van Gool (grant number 920-03-392).

Reference List

1 Cutler GB, Jr.: The role of estrogen in bone growth and maturation during childhood and adolescence. J Steroid Biochem Mol Biol 1997;61:141-144.

2 Grumbach MM: Estrogen, bone, growth and sex: a sea change in conventional wisdom. J Pediatr Endocrinol Metab 2000;13 Suppl 6:1439-1455.

3 Juul A: The effects of oestrogens on linear bone growth. Hum Reprod Update 2001;7:303-313.

4 Van der Eerden BC, Karperien M, Wit JM: The estrogen receptor in the growth plate: implications for pubertal growth. J Pediatr Endocrinol Metab 2001;14 Suppl 6:1527-1533.

5 Simm PJ, Bajpai A, Russo VC, Werther GA: Estrogens and growth. Pediatr Endocrinol Rev 2008;6:32-41.

6 Zirilli L, Rochira V, Diazzi C, Caffagni G, Carani C: Human models of aromatase deficiency. J Steroid Biochem Mol Biol 2008;109:212-218.

7 Dunkel L: Use of aromatase inhibitors to increase final height. Mol Cell Endocrinol 25-7-2006;254-255:207-216.

8 Shulman DI, Francis GL, Palmert MR, Eugster EA: Use of aromatase inhibitors in children and adolescents with disorders of growth and adolescent development. Pediatrics 2008;121:e975-e983.

9 Hero M, Norjavaara E, Dunkel L: Inhibition of estrogen biosynthesis with a potent aromatase inhibitor increases predicted adult height in boys with idiopathic short stature: a randomized controlled trial. J Clin Endocrinol Metab 2005;90:6396-6402.

10 Wickman S, Sipila I, Ankarberg-Lindgren C, Norjavaara E, Dunkel L: A specific aromatase inhibitor and potential increase in adult height in boys with delayed puberty: a randomised controlled trial. Lancet 2-6-2001;357:1743-1748.

11 Hero M, Wickman S, Dunkel L: Treatment with the aromatase inhibitor letrozole during adolescence increases near-final height in boys with constitutional delay of puberty. Clin Endocrinol (Oxf) 2006;64:510-513.

12 Mieszczak J, Lowe ES, Plourde P, Eugster EA: The aromatase inhibitor anastrozole is ineffective in the treatment of precocious puberty in girls with McCune-Albright syndrome. J Clin Endocrinol Metab 2008;93:2751-2754.

13 Feuillan P, Calis K, Hill S, Shawker T, Robey PG, Collins MT: Letrozole treatment of precocious puberty in girls with the McCune-Albright syndrome: a pilot study. J Clin Endocrinol Metab 2007;92:2100-2106.

14 Merke DP, Keil MF, Jones JV, Fields J, Hill S, Cutler GB, Jr.: Flutamide, testolactone, and reduced hydrocortisone dose maintain normal growth velocity and bone maturation despite elevated androgen levels in children with congenital adrenal hyperplasia. J Clin Endocrinol Metab 2000;85:1114-1120.

15 Simpson ER, Mahendroo MS, Means GD, Kilgore MW, Hinshelwood MM, Graham-Lorence S, Amarneh B, Ito Y, Fisher CR, Michael MD: Aromatase cytochrome P450, the enzyme responsible for estrogen biosynthesis. Endocr Rev 1994;15:342-355.

16 Yanovski JA, Rose SR, Municchi G, Pescovitz OH, Hill SC, Cassorla FG, Cutler GB, Jr.: Treatment with a luteinizing hormone-releasing hormone agonist in adolescents with short stature. N Engl J Med 6-3-2003;348:908-917.

17 Garcia-Segura LM: Aromatase in the brain: not just for reproduction anymore. J Neuroendocrinol 2008;20:705-712.

18 Goss PE, Qi S, Josse RG, Pritzker KP, Mendes M, Hu H, Waldman SD, Grynpas MD: The steroidal aromatase inhibitor exemestane prevents bone loss in ovariectomized rats. Bone 2004;34:384-392.

19 Van der Eerden BC, Emons J, Ahmed S, van Essen HW, Lowik CW, Wit JM, Karperien M: Evidence for genomic and nongenomic actions of estrogen in growth plate regulation in female and male rats at the onset of sexual maturation. J Endocrinol 2002;175:277-288.

20 Postnov AA, Vinogradov AV, Van Dyck D, Saveliev SV, De Clerck NM: Quantitative analysis of bone mineral content by x-ray microtomography. Physiol Meas 2003;24:165-178.

21 Waarsing JH, Day JS, van der Linden JC, Ederveen AG, Spanjers C, De Clerck N, Sasov A, Verhaar JA, Weinans H: Detecting and tracking local changes in the tibiae of individual rats: a novel method to analyse longitudinal *in vivo* micro-CT data. Bone 2004;34:163-169.

22 Feldkamp LA, Davis LC, Kress J.W: Practical cone-beam algorithm. J Opt Soc AM 1984;1:612-619.

23 De Clerck N, Postnov A: High resolution X-ray microtomography: Applications in biomedical research.; in Ntziachristos V, Leroy-Willig A, Tavitian B (eds): Textbook of *in vivo* imaging in vertebrates. Wiley, 2007, pp 57-77.

24 Sasov A, Van Dyck D: Desktop X-ray microscopy and microtomography. J Microsc 1998;191:151-158.

25 Weibel ER: in Academic Press (ed): Stereological methods. Vol.I. Practical methods for Biological Morphometry. London, 1979.

26 Buul-Offers SC, Reijnen-Gresnigt MG, Hoogerbrugge CM, Bloemen RJ, Kuper CF, Van den Brande JL: Recombinant insulin-like growth factor-II inhibits the growth-stimulating effect of growth hormone on the liver of Snell dwarf mice. Endocrinology 1994;135:977-985.

27 Turner RT, Riggs BL, Spelsberg TC: Skeletal effects of estrogen. Endocr Rev 1994;15:275-300.

28 Dupont S, Krust A, Gansmuller A, Dierich A, Chambon P, Mark M: Effect of single and compound knockouts of estrogen receptors alpha (ERalpha) and beta (ERbeta) on mouse reproductive phenotypes. Development 2000;127:4277-4291.

29 Oz OK, Zerwekh JE, Fisher C, Graves K, Nanu L, Millsaps R, Simpson ER: Bone has a sexually dimorphic response to aromatase deficiency. J Bone Miner Res 2000;15:507-514.

30 Oz OK, Hirasawa G, Lawson J, Nanu L, Constantinescu A, Antich PP, Mason RP, Tsyganov E, Parkey RW, Zerwekh JE, Simpson ER: Bone phenotype of the aromatase deficient mouse. J Steroid Biochem Mol Biol 2001;79:49-59.

31 Lindberg MK, Alatalo SL, Halleen JM, Mohan S, Gustafsson JA, Ohlsson C: Estrogen receptor specificity in the regulation of the skeleton in female mice. J Endocrinol 2001;171:229-236.

32 Chagin AS, Savendahl L: Oestrogen receptors and linear bone growth. Acta Paediatr 2007;96:1275-1279.

33 Turner KJ, Morley M, Atanassova N, Swanston ID, Sharpe RM: Effect of chronic administration of an aromatase inhibitor to adult male rats on pituitary and testicular function and fertility. J Endocrinol 2000;164:225-238.

34 Santen RJ, Lee JS, Wang S, Demers LM, Mauras N, Wang H, Singh R: Potential role of ultra-sensitive estradiol assays in estimating the risk of breast cancer and fractures. Steroids 7-7-2008.

35 Evans TR, di Salle E, Ornati G, Lassus M, Benedetti MS, Pianezzola E, Coombes RC: Phase I and endocrine study of exemestane (FCE 24304), a new aromatase inhibitor, in postmenopausal women. Cancer Res 1-11-1992;52:5933-5939.

36 Britt KL, Drummond AE, Dyson M, Wreford NG, Jones ME, Simpson ER, Findlay JK: The ovarian phenotype of the aromatase knockout (ArKO) mouse. J Steroid Biochem Mol Biol 2001;79:181-185.

37 Murata Y, Robertson KM, Jones ME, Simpson ER: Effect of estrogen deficiency in the male: the ArKO mouse model. Mol Cell Endocrinol 31-7-2002;193:7-12.

38 Jones ME, Thorburn AW, Britt KL, Hewitt KN, Misso ML, Wreford NG, Proietto J, Oz OK, Leury BJ, Robertson KM, Yao S, Simpson ER: Aromatase-deficient (ArKO) mice accumulate excess adipose tissue. J Steroid Biochem Mol Biol 2001;79:3-9.

39 Govoni KE, Wergedal JE, Chadwick RB, Srivastava AK, Mohan S: Prepubertal OVX increases IGF-I expression and bone accretion in C57BL/6J mice. Am J Physiol Endocrinol Metab 2008;295:E1172-E1180.

40 Kalu DN, Arjmandi BH, Liu CC, Salih MA, Birnbaum RS: Effects of ovariectomy and estrogen on the serum levels of insulin-like growth factor-I and insulin-like growth factor binding protein-3. Bone Miner 1994;25:135-148.

41 de Fougerolles NE, Greenstein B, Khamashta M, Hughes GR: Evidence for sexual dimorphism of estrogen receptors in hypothalamus and thymus of neonatal and immature Wistar rats. Int J Immunopharmacol 1999;21:869-877.

42 Goss PE, Qi S, Cheung AM, Hu H, Mendes M, Pritzker KP: Effects of the steroidal aromatase inhibitor exemestane and the nonsteroidal aromatase inhibitor letrozole on bone and lipid metabolism in ovariectomized rats. Clin Cancer Res 1-9-2004;10:5717-5723.

43 Manolagas SC: Birth and death of bone cells: basic regulatory mechanisms and implications for the pathogenesis and treatment of osteoporosis. Endocr Rev 2000;21:115-137.

44 Sinha S, Kaseta J, Santner SJ, Demers LM, Bremmer WJ, Santen RJ: Effect of CGS 20267 on ovarian aromatase and gonadotropin levels in the rat. Breast Cancer Res Treat 1998;48:45-51.

45 Adashi EY, Hennebold JD: Single-gene mutations resulting in reproductive dysfunction in women. N Engl J Med 4-3-1999;340:709-718.

46 Rosenfeld CS, Wagner JS, Roberts RM, Lubahn DB: Intraovarian actions of oestrogen. Reproduction 2001;122:215-226.

47 McEwen B: Estrogen actions throughout the brain. Recent Prog Horm Res 2002;57:357-384.

48 Veiga S, Azcoitia I, Garcia-Segura LM: Ro5-4864, a peripheral benzodiazepine receptor ligand, reduces reactive gliosis and protects hippocampal hilar neurons from kainic acid excitotoxicity. J Neurosci Res 1-4-2005;80:129-137.

49 Azcoitia I, Sierra A, Veiga S, Honda S, Harada N, Garcia-Segura LM: Brain aromatase is neuroprotective. J Neurobiol 15-6-2001;47:318-329.

50 Carswell HV, Dominiczak AF, Garcia-Segura LM, Harada N, Hutchison JB, Macrae IM: Brain aromatase expression after experimental stroke: topography and time course. J Steroid Biochem Mol Biol 2005;96:89-91.

51 Garcia-Segura LM, Wozniak A, Azcoitia I, Rodriguez JR, Hutchison RE, Hutchison JB: Aromatase expression by astrocytes after brain injury: implications for local estrogen formation in brain repair. Neuroscience 1999;89:567-578.

52 Veiga S, Azcoitia I, Garcia-Segura LM: Extragonadal synthesis of estradiol is protective against kainic acid excitotoxic damage to the hippocampus. Neuroreport 28-9-2005;16:1599-1603.

53 Johansen JA, Jordan CL, Breedlove SM: Steroid hormone masculinization of neural structure in rats: a tale of two nuclei. Physiol Behav 15-11-2004;83:271-277.

54 Morishima A, Grumbach MM, Simpson ER, Fisher C, Qin K: Aromatase deficiency in male and female siblings caused by a novel mutation and the physiological role of estrogens. J Clin Endocrinol Metab 1995;80:3689-3698.